Article

Novel TREM-1 Inhibitors Attenuate Tumor Growth and Prolong Survival in Experimental Pancreatic Cancer

Zu T. Shen, and Alexander B. Sigalov

Mol. Pharmaceutics, **Just Accepted Manuscript** • DOI: 10.1021/acs.molpharmaceut.7b00711 • Publication Date (Web): 02 Nov 2017

Novel TREM-1 Inhibitors Attenuate Tumor Growth and Prolong Survival in Experimental Pancreatic Cancer

Zu T. Shen, Alexander B. Sigalov*

SignaBlok, Inc, P.O. Box 4064, Shrewsbury, MA 01545, United States of America

* Corresponding author: Alexander B. Sigalov

SignaBlok, Inc, P.O. Box 4064, Shrewsbury, MA 01545, United States of America.

Phone: 203-505-3807

E-mail: sigalov@signablok.com

ABSTRACT

Pancreatic cancer (PC) is a highly lethal cancer with an urgent need to expand the limited treatment options for patients. Tumor-associated macrophages (TAMs) promote tumor aggressiveness and metastasis. High expression of triggering receptor expressed on myeloid cells 1 (TREM-1) on TAMs directly correlates with poor survival in patients with non-small cell lung cancer (NSCLC). We have previously hypothesized that blockade of TREM-1 could be a promising therapeutic strategy to treat cancer and shown that the novel, ligand-independent TREM-1 inhibitory peptides rationally designed using the signaling chain homooligomerization (SCHOOL) strategy suppress NSCLC growth *in vivo*. Here, we evaluated the therapeutic potential of these inhibitors in three human PC xenograft mouse models. Administration of SCHOOL peptides resulted in a strong antitumor effect achieving an optimal treatment/control (T/C) value of 19% depending on the xenograft and formulation used and persisting even after treatment was halted. The effect correlated significantly with increased survival and suppressed TAM infiltration. The peptides were well-tolerated when deployed in either free form or formulated into lipopeptide complexes for peptide half-life extension and targeted delivery. Finally, blockade of TREM-1 significantly reduced serum levels of interleukin (IL)-1α, IL-6 and macrophage colony-stimulating factor (M-CSF), but not vascular endothelial growth factor, suggesting M-CSF-dependent antitumor mechanisms. Collectively, these promising data suggest that SCHOOL TREM-1-specific peptide inhibitors have a cancer type-independent, therapeutically beneficial antitumor activity and can be potentially used as a stand-alone therapy or as a component of combinational therapy for PC, NSCLC, and other solid tumors.

KEYWORDS: Triggering Receptor Expressed on Myeloid Cells 1; Tumor-Associated Macrophages; SCHOOL Model of Cell Signaling; SCHOOL Inhibitory Peptides; Targeted Delivery

INTRODUCTION

Pancreatic cancer (PC, 85% of which are pancreatic ductal adenocarcinomas, PDAC) is the fourth leading cause of cancer-related mortality across the world with very poor clinical outcome.[1] Current treatments of PC all only marginally prolong survival or relieve symptoms in patients with PC.[2] There has been no significant progress in the field of targeted therapy for PC[3] and despite tremendous efforts, the 5-year survival rate remains less than 5%.[4]

As many other solid tumors, PC is characterized by a marked infiltration of macrophages into the stromal compartment,[5-6] a process, which is mediated by cancer-associated fibroblasts (CAFs) (Figure 1A) and plays a key role in disease progression and its response to therapy. These tumor-associated macrophages (TAMs) secrete a variety of growth factors, cytokines, chemokines, and enzymes that regulate tumor growth, angiogenesis, invasion, and metastasis.[5, 7-8] High macrophage infiltration correlates with the promotion of tumor growth and metastasis development.[6, 9-10] In patients with PC, macrophage infiltration begins during the pre-invasive stage of the disease and increases progressively.[11] The number of TAMs is significantly higher in patients with metastases.[12] Presence of TAMs in the PC stroma correlates with increased angiogenesis,[13] a known predictor of poor prognosis.[14] TAM recruitment, activation, growth and differentiation are regulated by macrophage colony-stimulating factor (M-CSF, also known as colony-stimulating factor 1, CSF-1).[15-16] High pretreatment serum M-CSF is a strong independent predictor of poor survival in PC patients.[17] In PC mouse models, blockade of M-CSF or its receptor not only suppresses tumor angiogenesis and lymphangiogenesis[18] but also improves response to T-cell checkpoint immunotherapies that target programmed cell death protein 1 (PD-1) and cytotoxic T lymphocyte antigen-4 (CTLA-4).[19] Importantly, continuous M-CSF inhibition affects only pathological angiogenesis but not healthy vascular and lymphatic systems outside tumors.[18] In contrast to blockade of vascular endothelial growth factor (VEGF), interruption of M-CSF

inhibition does not promote rapid vascular regrowth.[18] Collectively, these findings further suggest that targeting TAMs is a promising strategy for treating cancer.[20-22]

Triggering receptor expressed on myeloid cells-1 (TREM-1) amplifies the inflammatory response[23] and is upregulated under inflammatory conditions including acute pancreatitis.[24] TREM-1 activation enhances release of multiple cytokines including monocyte chemoattractant protein-1 (MCP-1), tumor necrosis factor-α (TNFα), interleukin-1α (IL-1α), IL-1β, IL-6 and M-CSF.[25-27] Most of these cytokines are increased in patients with PC[28-29] and play a vital role in creating and sustaining inflammation in the tumor favorable microenvironment, thus affecting patient survival. Inhibition of TREM-1 lowers levels of proinflammatory cytokines and is a promising approach in a variety of inflammation-associated disorders.[23, 26-27, 30-31] Importantly, in contrast to cytokine blockers, blockade of TREM-1 can blunt excessive inflammation while preserving the capacity for microbial control.[32] *In vitro* silencing of TREM-1 suppresses cancer cell invasion.[33] In patients with non-small cell lung cancer (NSCLC), TREM-1 expression on TAMs is associated with cancer recurrence and poor survival: patients with low TREM-1 expression have a 4-year survival rate of over 60%, compared with less than 20% in patients with high TREM-1 expression.[33]

We have previously shown that blockade of TREM-1 attenuates the specific inflammatory response *in vitro* and *in vivo* and inhibits tumor growth in two xenograft mouse models of NSCLC.[27] Despite some recent evidence that peptidoglycan (PGN) recognition protein 1 (PGLYRP1) may potentially act as a ligand for TREM-1,[34] the actual nature of the TREM-1 ligand(s) and mechanisms of TREM-1 signaling are still unknown. For this reason, we used a new model of transmembrane signaling, the signaling chain homooligomerization (SCHOOL) model,[35-36] to rationally design a TREM-1-specific inhibitory nonapeptide GF9 that employs a novel, ligand-independent mechanism of TREM-1 inhibition by blocking the

interaction of TREM-1 with DAP-12 in the membrane (Figure 1B).[27] We also formulated GF9 into self-assembling lipopeptide complexes that mimic human high density lipoproteins (HDL) for peptide half-life extension and targeted delivery to macrophages (Figure 1B). We showed that this incorporation decreases the effective peptide dose in mice with NSCLC xenografts[27] and collagen-induced arthritis (CIA).[31]

In the present study, we evaluate the therapeutic potential of GF9 in the BxPC-3, AsPC-1 and Capan-1 xenograft mouse models of PC. We also use peptides GE31 and GA31, both of which contain the GF9 sequence combined with sequences from either helix 4 or 6 of the major HDL protein, apolipoprotein (apo) A-I, respectively. By combining these sequences, GA31 and GE31 are able to perform three functions: assist in the self-assembly of HDL, target HDL to macrophages and inhibit TREM-1. The free and HDL-bound TREM-1-specific inhibitory peptide sequences studied exhibit a strong antitumor effect, which persists even after treatment is halted and correlates significantly with increased survival and suppressed TAM infiltration. Blockade of TREM-1 significantly reduces serum levels of IL-1α, IL-6 and M-CSF, but not VEGF, suggesting M-CSF-dependent antitumor mechanisms. Collectively, these promising data suggest that these well-tolerated peptide inhibitors of TREM-1 have a cancer type-independent, therapeutically beneficial antitumor activity and can be potentially used as a stand-alone therapy or as a component of combinational therapy for PC, NSCLC, and other solid tumors including brain tumors.

EXPERIMENTAL SECTION

Cell lines and reagents. Human pancreatic cancer cell lines (AsPC-1, BxPC-3, and Capan-1) were purchased from the ATCC. Sodium cholate, cholesteryl oleate and other chemicals were purchased from Sigma Aldrich Company. 1,2-dimyristoyl-*sn*-glycero-3-phosphocholine (DMPC), 1,2-dimyristoyl-*sn*-glycero-3-phospho-(1′-rac-glycerol) (DMPG), 1-palmitoyl-2-oleoyl-sn-glycero-3-phosphocholine (POPC), 1-palmitoyl-2-oleoyl-*sn*-glycero-3-phospho-(1'-rac-glycerol) (POPG), 1,2-dimyristoyl-*sn*-glycero-3-phosphoethanolamine-N-(lissamine rhodamine B sulfonyl) (Rho B-PE) and cholesterol were purchased from Avanti Polar Lipids.

Peptide synthesis. The following synthetic peptides were ordered from Bachem Americas, Inc.: one 9-mer peptide GFLSKSLVF (human TREM-$1_{213-221}$, GF9), two 22-mer methionine sulfoxidized peptides PYLDDFQKKWQEEM(O)ELYRQKVE (H4) and PLGEEM(O)RDRARAHVDALRTHLA (H6) that correspond to human apo A-I helices 4 (apo A-$I_{123-144}$) and 6 (apo A-$I_{167-188}$), respectively, and two 31-mer methionine sulfoxidized peptides, GFLSKSLVFPYLDDFQKKWQEEM(O)ELYRQKVE (GE31) and GFLSKSLVFPLGEEM(O)RDRARAHVDALRTHLA (GA31).

Lipopeptide complexes. HDL-mimicking lipopeptide complexes of discoidal (dHDL) and spherical (sHDL) morphology loaded with GF9 (GF9-dHDL and GF9-sHDL, respectively) or an equimolar mixture of GA31 and GE31 (GA/E31-dHDL and GA/E31-sHDL) were synthesized using the sodium cholate dialysis procedure, purified and characterized essentially as previously described.[27, 31, 37] Briefly, in discoidal complexes, the molar ratio was 65:25:3:1:190 corresponding to POPC:POPG:GF9:apo A-I:sodium cholate for GF9-dHDL that contain GF9 and an equimolar mixture of oxidized apo A-I peptides H4 and H6 peptides or 65:25:1:190 corresponding to DMPC:DMPG:GA/E31:sodium cholate for

GA/E31-dHDL that contain an equimolar mixture of oxidized peptides GA31 and GE31. In spherical complexes, the molar ratio was 125:6:2:3:1:210 corresponding to POPC:cholesterol:cholesteryl oleate:GF9:apo A-I:sodium cholate for GF9-sHDL that contain GF9 and an equimolar mixture of oxidized apo A-I peptides H4 and H6 or 125:6:2:1:210 corresponding to POPC:cholesterol:cholesteryl oleate:GA/E31:sodium cholate for GA/E31-sHDL that contain an equimolar mixture of oxidized peptides GA31 and GE31.

Mouse xenograft tumor models. All animal studies were performed by Bolder BioPATH and conducted under an approved IACUC protocol. Briefly, 5-6 week old female athymic nude-Foxn1^{nu} mice were obtained from Envigo (formerly Harlan, Inc.). Mice were implanted subcutaneously into the right flank with 5x10^6 AsPC-1, BxPC-3 or Capan-1 cells in equal parts of serum-free growth medium and Matrigel. Mice were monitored daily and tumor measurements were taken along the length and width using Vernier calipers twice weekly until sacrifice. Tumor volumes were calculated using a modified ellipsoidal formula: (Length x Width^2) / 2. When tumors reached a calculated volume of approximately 150-200 mm^3, mice were sorted into treatment groups and injected intraperitoneally (i.p.) once daily for 5 days per week (5qw) with free or HDL-bound TREM-1 inhibitory GF9 sequences: GF9 (2.5 and 25 mg/kg), GF9-dHDL (2.5 mg/kg), GF9-sHDL (2.5 mg/kg), GA/E31-dHDL (dose equivalent to 4 mg of GF9/kg), and GA/E31-sHDL (dose equivalent to 4 mg of GF9/kg) or with PBS. Treatment persisted for 31 days, 29 days and 29 days for mice containing established AsPC-1, BxPC-3 and Capan-1 xenograft tumors, respectively. Mice were humanely sacrificed when individual tumors exceeded 1500 mm^3.

Immunohistochemistry. All staining and quantification procedures were performed by HistoTox Labs. Briefly, mice containing AsPC-1, BxPC-3 and Capan-1 tumors were humanely euthanized for necropsy at the end of the study. Excised tumors were fixed using 10% neutral buffered formalin for 1-2 days, processed for paraffin embedding and sectioned

at 4 μm. Antigen retrieval for F4/80 was achieved using Proteinase K (Dako North America). Sections were blocked for perioxidase and alkaline phosphatase activity using Dual Endogenous Enzyme Block (Dako North America). Sections were then incubated with Protein Block (Dako North America) followed by primary antibody F4/80 (1:2000, AbD Serotec) diluted using 1% bovine serum albumin in Tris-buffered saline. Afterwards, sections were incubated using EnVision+ secondary antibodies (Dako North America), followed by 3,3'-diaminobenzidine in chromogen solution (Dako North America) and counterstained using hematoxylin (Dako North America). Quantitative analysis of intratumoral F4/80 staining was determined using Visiopharm software.

Cytokine detection. Blood was collected on study days 1 and 8 and processed into serum. Serum cytokines were analyzed by Quantibody Mouse Cytokine Array Q1 kits (RayBiotech) according to the manufacturer's instructions.

Statistical analysis. All statistical analyses were performed using GraphPad Prism 6.0 (GraphPad Software). Percent treatment/control (T/C) values were calculated using the following formula: % T/C = 100 x $\Delta T/\Delta C$ where T and C are the mean tumor volumes of the drug-treated and control groups, respectively, on the final day of the treatment; ΔT is the mean tumor volume of the drug-treated group on the final day of the treatment minus mean tumor volume of the drug-treated group on initial day of dosing; and ΔC is the mean tumor volume of the control group on the final day of the treatment minus mean tumor volume of the control group on initial day of dosing.

Results are expressed as the mean ± SEM. Statistical differences were analyzed using analysis of variance with Bonferroni adjustment unless otherwise noted. The Kaplan-Meier method was used to estimate survival as a function of time, and survival differences were analyzed by the log-rank test. *p* values less than 0.05 were considered significant.

Sequence accession numbers. Accession numbers (UniProtKB/Swiss-Prot knowledgebase, http://www.uniprot.org/) for the protein sequences discussed in this Research Article is as the follows: human TREM-1, Q9NP99; human apo A-I, P02647.

RESULTS

SCHOOL TREM-1 inhibitory GF9 sequences exhibit single-agent antitumor activity and prolong survival in BxPC-3, AsPC-1, and Capan-1 xenograft mouse models. Previously, we reported that oxidation of apo A-I or its peptides H4 and H6 significantly enhances targeted delivery of SCHOOL TREM-1 inhibitory GF9 sequences or imaging agents incorporated into HDL-mimicking lipopeptide complexes to macrophages *in vitro* and *in vivo*.[27, 37-39] We also demonstrated that free and HDL-bound GF9 exhibits single-agent antitumor activity in H292 and A549 xenograft models of NSCLC and hypothesized that this TAM-targeted antitumor strategy is cancer type-independent.[27] This prompted us to extend our previous work and test the *in vivo* efficacy of GF9, GF9-HDL and GA31+GE31 in an equimolar ratio (GA/E31)-HDL in BxPC-3, AsPC-1, and Capan-1 xenograft models of PC in nude mice.

When administered daily at a dose of 25 mg/kg, free GF9 showed antitumor efficacy in all three models studied (Figure 2A), with the effect most pronounced in the Capan-1 model (31% T/C) compared with the BxPC-3 and AsPC-1 models (41 and 56% T/C, respectively). The observed antitumor effect of 25 mg/kg GF9 is dose-dependent and specific: administration of GF9 at 2.5 mg/kg or a control peptide GF9-G at 25 mg/kg did not affect tumor growth (not shown).

To test whether targeted delivery of GF9 to macrophages by formulation of GF9 into macrophage-targeted lipopeptide complexes of either discoidal (dHDL) or spherical (sHDL) reduces the effective peptide dose, GF9-dHDL and GF9-sHDL were administered daily at 2.5

mg of GF9/kg. Despite a 10-fold decrease in administration dose of GF9, the observed therapeutic effect of GF9-HDL was comparable (42, 40, and 28% T/C as observed for GF9-dHDL in AsPC-1, BxPC-3, and Capan-1, respectively) or even better (26% T/C as observed for GF9-sHDL in BxPC-3) than that observed for GF9 at 25 mg/kg (Figure 2A). Further, we have previously shown that peptides GE31 and GA31 with sequences from GF9 and apo A-I helices 4 and 6 are able to perform three functions: assist in the self-assembly of HDL, target HDL to macrophages and silence the TREM-1 signaling pathway in mice with CIA.[31] To address the question of whether these SCHOOL TREM-1 inhibitory GF9 sequences formulated into HDL-mimicking macrophage-targeted lipopeptide complexes can provide antitumor efficacy *in vivo*, we administered either GA/E31-dHDL or GA/E31-sHDL at a dose equivalent to 4 mg/kg GF9 and found that GA/E31-HDL inhibited tumor growth in all three xenograft models (Figure 3A) with activity comparable or even better (19 and 21% T/C as observed for GA/E31-dHDL in BxPC-3 and Capan-1, respectively) than that observed for GF9-HDL at 2.5 mg/kg (Figure 2A). Kaplan-Meier survival curves demonstrated that treatment with free or HDL-bound SCHOOL TREM-1 inhibitory GF9 sequences significantly prolonged survival relative to vehicle control in all three xenograft models of PC studied (Figure 4). Collectively, these findings suggest that incorporation of GF9 alone or as a part of GE31 and GA31 peptides into macrophage-specific lipopeptide complexes reduces the effective peptide dose up to 10-fold probably due to improved pharmacokinetic parameters of the peptide and its targeted delivery. In addition, the antitumor activity demonstrated by GA/E31-HDL (Figures 3 and 4) further confirms our previous findings regarding the multifunctionality of these peptide sequences.[31] It should be also noted that in all xenograft mouse models of PC studied, daily administration of free or HDL-bound SCHOOL TREM-1 inhibitory GF9 sequences for 5 consecutive days per week for more than 4 weeks did not cause any loss in the animal weight (Figures 2B and 3B), and there was no

obvious sign of toxicity during the course of the treatment. This further confirms our previous findings that free and HDL-bound GF9 are well-tolerated by healthy mice and H292 and A549 tumor-bearing mice.[27] In summary, these data collectively not only provide the first *in vivo* experimental evidence of the potential involvement of TREM-1-regulated pathway in PC, thereby implicating the potential of TREM-1 inhibitors as novel antitumor agents for the treatment of PC, but also support the previously predicted cancer type-independent mechanisms of antitumor activity of SCHOOL TREM-1 inhibitory GF9 sequences.[27] Formulation of these sequences into macrophage-specific self-assembling lipopeptide complexes that mimic human HDL substantially increases their therapeutic efficacy probably because of targeted delivery and/or the half-life extension of the peptides in circulation afforded by this strategy.

SCHOOL TREM-1 inhibitory GF9 sequences suppress macrophage infiltration into the tumor. The *in vivo* biologic effects of SCHOOL TREM-1 inhibitory GF9 sequences were further addressed by histological and immunohistochemical (IHC) studies. To investigate immune infiltration into the tumor microenvironment and address whether macrophages were reduced in BxPC-3-, AsPC-1-, and Capan-1-bearing mice treated with GF9, GF9-HDL and GA/E31-HDL, we performed IHC analysis using the murine macrophage marker F4/80. In vehicle-treated mice, IHC analysis revealed that intratumoral macrophage infiltration depended on the PC xenograft line: significantly higher macrophage infiltration (up to 20%) was observed in BxPC-3 and Capan-1 tumors compared with that in AsPC-1 tumors (less than 5%) (data not shown). To establish a correlation between the anticancer effect of the TREM-1 treatments used and TAM content, we plotted the calculated anticancer activity (% T/C) from groups of BxPC-3-, AsPC-1-, and Capan-1-bearing mice treated using free and HDL-bound SCHOOL TREM-1 inhibitory GF9 sequences against the intratumoral macrophage content and observed that the higher the intratumoral macrophage

content, the higher was the antitumor activity of the tested SCHOOL TREM-1 inhibitory GF9 sequences (Figure 5A). We also found that treatment with SCHOOL TREM-1 inhibitory GF9 sequences substantially reduced macrophage content in tumors of BxPC-3-bearing mice compared with control (Figures 5B and 5C). One may suggest that testing a tumor for its inflammation status can help to identify those patients who will better respond to TREM-1-targeted therapy. In summary, these findings show for the first time that TREM-1 inhibition reduces macrophage infiltration into xenograft tumors.

SCHOOL TREM-1 inhibitory GF9 sequences inhibit the release of proinflammatory cytokines and M-CSF. M-CSF and proinflammatory cytokines such as IL-1α and IL-6 are involved in tumor angiogenesis and PC invasiveness.[17-18, 28-29] Previously, we observed that TREM-1 inhibition using free and HDL-bound SCHOOL TREM-1 inhibitory GF9 sequences reduces the production of proinflammatory cytokines and M-CSF in septic mice[27] and mice with CIA.[31] In this study, to further elucidate the molecular mechanisms underlying the observed anticancer effect of SCHOOL TREM-1 inhibitory GF9 sequences, we investigated whether TREM-1 inhibition using GF9, GF9-HDL and GA/E31-HDL affects the release of proinflammatory cytokines and M-CSF in BxPC-3-, AsPC-1-, and Capan-1-bearing mice. We analyzed serum cytokine levels on study days 1 and 8 and found that administration of free GF9 at 25 mg/kg and GF9-sHDL at 2.5 mg/kg inhibits the production of IL-1α (except of AsPC-1), IL-6, and M-CSF compared with vehicle-treated mice (Figure 6; shown for GF9 and GF9-sHDL). Similar data were obtained for GA/E31-HDL (not shown). The effect is dose-dependent and specific: GF9 at 2.5 mg/kg and GF9-G at 25 mg/kg did not affect the release of either cytokines or M-CSF (not shown). Collectively, these data indicate that inhibition of the TREM-1 signaling pathway using free and HDL-bound SCHOOL TREM-1 inhibitory GF9 sequences reduces the release of proinflammatory cytokines and M-CSF in experimental PC.

DISCUSSION

To the best of our knowledge, this study is the first report showing the *in vivo* efficacy of novel, ligand-independent SCHOOL TREM-1 inhibitory GF9 sequences in free form (GF9) and formulated into macrophage-specific lipopeptide complexes (GF9-HDL and GA/E31-HDL) in PC. This not only extends our previous observations that free and HDL-bound GF9 exhibit the *in vivo* anticancer efficacy in NSCLC[27] but, importantly, suggests that the therapeutic effect of our TREM-1-targeted treatment is cancer type-independent. The major findings in the present study are that administration of GF9, GF9-HDL, and GA/E31-HDL results in a strong antitumor effect achieving an optimal T/C value of 19% depending on the xenograft and formulation used and persisting even after treatment was halted (Figures 2A and 3A). We also demonstrate that mice treated with these TREM-1 inhibitors show substantially prolonged survival in comparison to the control (Figure 4). These and our previous data[27] are in line with the observed three-fold increase in the 4-year survival rate in NSCLC patients with low TREM-1 expression on TAMs compared with those with high TREM-1 expression.[33] Therefore, the obtained results provide significant proof of concept that SCHOOL TREM-1 inhibitory GF9 sequences that can inhibit TREM-1 in a ligand-independent manner may have potential as a new TAM-targeted treatment for solid tumors. This treatment can be potentially used as a stand-alone therapy or as a component of combinational therapy.

Interestingly, GF9, GF9-HDL, and GA/E31-HDL all inhibit tumor growth and prolong survival in BxPC-3, AsPC-1, and Capan-1 xenografts (Figures 2, 3, and 4) suggesting that GF9 can reach its intramembrane site of action from either outside (free GF9, Route 1, Figure 1B) or inside the cell (GF9-HDL and GA/E31-HDL, Route 2, Figure 1B). Further, the beneficial antitumor effect of TREM-1 inhibitory GF9 sequences either in free or HDL-

bound form continues after cessation of treatment (Figures 2 and 3). This suggests that once delivered to its site of action, GF9 or GF9-containing peptide sequence can remain in the membrane and inhibit TREM-1. *In vivo* half-life extension of GF9 incorporated into HDL as GF9 alone or as a part of GE31 and GA31 peptides (Zu Shen and Alexander Sigalov, unpublished data) may also contribute to the observed effect: while the peptide half-life *in vivo* is short, typically a few minutes,[40] discoidal (or nascent) HDL and sHDL are known to have half-lives of 12-20 hrs and 4-5 days, respectively.[41]

TAMs facilitate a microenvironment that promotes tumor development and are an important drug target for cancer therapy.[10, 42] An increased level of macrophage infiltration into tumors correlates with increased angiogenesis and poor prognosis.[42] By promoting tumor angiogenesis, TAMs play an important role in the tumor progression to malignancy. Inhibition of intratumoral macrophage infiltration delays the angiogenic switch and the malignant transition.[10] In this study, we found that blockade of TREM-1 inhibits macrophage infiltration in BxPC-3 tumors (Figure 5). Interestingly, the antitumor activity of SCHOOL TREM-1 inhibitory GF9 sequences as assessed by tumor size and survival of AsPC-1-, BxPC-3-, and Capan-1-bearing mice correlated with the intratumoral macrophage content observed in these xenograft models treated with vehicle alone. This suggests that TAM content may represent a biomarker that may help to identify those patients who will better respond to TREM-1-targeted therapy. This biomarker could be also used as a criterion for either including or excluding trial participants.

Myeloid cells are known to contribute directly to tumor angiogenesis and lymphangiogenesis by secreting multiple angiogenic factors including VEGF and M-CSF, which play a key role in cancer pathogenesis.[18, 43] Thus, one of the potential mechanisms underlying the *in vivo* anticancer activity of TREM-1 inhibitors observed in this study can be partly mediated through M-CSF inhibition, resulting in suppression of not only macrophage

infiltration into tumor sites but also angiogenesis. In mice with osteosarcoma, inhibition of M-CSF selectively suppresses tumor angiogenesis and lymphangiogenesis.[18] In line with these findings, our preliminary data (Zu Shen and Alexander Sigalov, unpublished observations) indicate that treatment with SCHOOL TREM-1 inhibitory GF9 sequences substantially reduced the number of blood vessels within the tumor as revealed by IHC analysis of the tumors from control and treated animals for microvessel density using CD31, or platelet endothelial cell adhesion molecule-1 (PECAM-1), as a marker to evaluate neovascularization in tumor xenografts.[44] Importantly, in contrast to blockade of VEGF that damages healthy vessels and promotes rapid vascular regrowth,[45] continuous inhibition of M-CSF does not affect healthy vascular and lymphatic systems outside tumors and is currently considered as a promising therapeutic strategy for targeting angiogenesis in cancer and ocular neovascular diseases.[18] In this study, we observed reduction of serum M-CSF but not VEGF in human PC tumor-bearing mice treated with either free or HDL-bound SCHOOL TREM-1 inhibitory GF9 sequences compared to vehicle-treated mice (Figure 6) or mice treated with GF9-G (not shown). Consistent with a recent report,[18] interruption of M-CSF inhibition via cessation of TREM-1 treatment does not result in rapid tumor regrowth in all xenografts studied (Figures 2A and 3A). Our current results are also in line with our previous data that demonstrate that in mice with CIA, treatment with SCHOOL TREM-1 inhibitory GF9 sequences results in reduced serum levels of M-CSF.[31] This also correlates well with our recent findings that in mice with oxygen-induced retinopathy (OIR), treatment with SCHOOL TREM-1 inhibitory GF9 sequences significantly reduces retinal expression of TREM-1 and prevents retinal neovascularization (Modesto Rojas, Zu Shen, Ruth Caldwell, Alexander Sigalov; unpublished data). Collectively, these data strongly support the hypothesis that TREM-1 blockade-mediated inhibition of M-CSF can contribute to the anticancer activity of TREM-1 inhibitors observed in this and a previous study.[27]

Our study shows that blockade of TREM-1 specifically suppresses key cytokines such as IL-1α, IL-6 and M-CSF, which are upregulated in PC and contribute to poor prognosis.[28, 46] In patients with PC, high IL-1α expression has been found to correlate poorly with clinical outcome and the patient's survival time.[29] By targeting CAFs, IL-1α plays a pivotal role in sustaining the PC tumor inflammatory microenvironment that supports tumor growth and progression and the recruitment of leukocytes such as macrophages.[13, 29] Thus, the suppression of IL-1α observed in this study is likely due to blockade of TREM-1 expressed on TAMs and subsequent disruption of the TAM-CAF network (Figure 1). Another key player in the tumor microenvironment, IL-6, promotes tumorigenesis by regulating apoptosis, survival, proliferation, angiogenesis, invasiveness and metastasis, and, most importantly, metabolism.[46] These considerations, together with the fact that IL-1α plays an important role in tumor-mediated angiogenesis, TREM-1 inhibition-mediated reduction of IL-1α and IL-6 may represent another mechanism of the antitumor activity of TREM-1 inhibitory GF9 sequences demonstrated in the present study.

One of the interesting opportunities that this study offers is to test the hypothesis that a combinatorial therapy for treating PC that includes first-line cytotoxic therapy (e.g., gemcitabine, GEM) and TREM-1 treatment that targets the tumor inflammatory microenvironment can not only synergistically improve survival of PC patients but also reduce recurrence risk. Interestingly, it was recently reported that GEM treatment increases TAM infiltration into PDAC tumors.[47] On the other hand, while targeting TAMs via inhibition of M-CSF (CSF-1) receptor only modestly slows tumor growth but decreases the number of tumor-initiating cells (TIC) in pancreatic tumors, combination of GEM with M-CSF receptor inhibitors synergistically increases chemotherapeutic efficacy, dramatically slows PC progression and blocks metastasis by the combined action of reducing TIC content.[47] Here, it should be noted that compared to normal pancreas, PDAC tissues are

known to express 3.7-fold more scavenger receptor (SR) class B member 1 (SR-B1),[48] which is normally expressed in the liver and functions as a receptor for HDL. Thus, in addition to targeting macrophages (including TAMs) by receptor (likely via SR class A, SR-A)-mediated uptake that involves methionine-sulfoxidized sites of the apo A-I helices 4 and 6, HDL-like lipopeptide complexes may also target PDAC cells via SR-B1-mediated uptake that involves potential SR-B1 epitopes located on the apo A-I helices 4 and 6.[49] This could allow the use of this lipopeptide platform to deliver not only TREM-1 therapy but also cytotoxic agents in a combinatorial therapy for PC. Further studies are needed to confirm this hypothesis.

Intriguingly, like other peptides that utilize the SCHOOL approach,[37, 50-51] TREM-1 inhibitory GF9 sequences self-insert into the plasma membrane from either outside or inside the cell (Figure 1B, Routes 1 and 2, respectively) and disconnect TREM-1 from DAP-12[27, 31] in a manner similar to that used by different viruses to suppress the host immune response.[37, 52] Together with the present study, this further supports our unifying hypothesis [37, 52] that these viral strategies developed and optimized during millions of years of evolution of virus-host interactions can be rationally used in the development of novel therapies.

CONCLUSION

The present study demonstrates that novel SCHOOL TREM-1 inhibitory GF9 sequences potently inhibit PC tumor growth and prolong survival in human PC tumor-bearing mice. To our knowledge, this study is the first to demonstrate the potential role of TREM-1 as a therapeutic target in PC treatment and to suggest suppression of the specific inflammatory response through silencing the TREM-1-mediated signaling pathway using TREM-1 peptide inhibitors designed using the SCHOOL approach as a novel therapeutic strategy against PC. Future studies are needed for testing these inhibitors in combination with chemotherapy and radiotherapy aiming to overcome the intrinsic and acquired resistance of PC cells, to enhance

the treatment efficacy, and to reduce PC patient's short-and long-term risks of recurrence and progression.

Our data provide further *in vivo* evidence in support of M-CSF- and cytokine-mediated molecular mechanisms underlying the tumor growth-inhibiting effect of these inhibitors in free or HDL-bound form observed in PC (this study) and NSCLC.[27] This further suggests that SCHOOL TREM-1 inhibitory GF9 sequences have a cancer type-independent, therapeutically beneficial antitumor activity and can be potentially used as a stand-alone therapy or as a component of combinational therapy for PC, NSCLC, and potentially other solid tumors (e.g., breast and colon cancer). In conjunction with the ability of the HDL-like lipopeptide complexes used in this study to cross the blood-brain barrier (Zu Shen and Alexander Sigalov, unpublished observations), this therapy can be potentially used to treat brain tumors such as glioblastoma, as well.

ACKNOWLEDGEMENTS

We are grateful to Bolder BioPATH for the animal experiments and HistoTox Labs, Inc. for the immunohistochemistry. We also owe a debt of gratitude to Dr. Dave Emerson who did an excellent job conducting mouse studies, for his important expertise, experience, and skills and for numerous valuable discussions. This work was partly supported by the National Cancer Institute of the National Institutes of Health under grant number R43CA195684 (ZTS, ABS; Alexander B. Sigalov, Principal investigator). The additional funding (ABS) has come from SignaBlok, Inc.

CONFLICT OF INTEREST DISCLOSURE

The authors declare no competing financial interest.

REFERENCES

(1) Hariharan, D.; Saied, A.; Kocher, H. M. Analysis of mortality rates for pancreatic cancer across the world. *HPB (Oxford)* **2008,** *10*, (1), 58-62.

(2) Schneider, G.; Siveke, J. T.; Eckel, F.; Schmid, R. M. Pancreatic cancer: basic and clinical aspects. *Gastroenterology* **2005,** *128*, (6), 1606-25.

(3) Walker, E. J.; Ko, A. H. Beyond first-line chemotherapy for advanced pancreatic cancer: an expanding array of therapeutic options? *World J Gastroenterol* **2014,** *20*, (9), 2224-36.

(4) American Cancer Society: Cancer Facts and Figures 2010. *American Cancer Society, Atlanta, GA* **2010**.

(5) Shih, J.-Y.; Yuan, A.; Chen, J. J.-W.; Yang, P.-C. Tumor-Associated Macrophage: Its Role in Cancer Invasion and Metastasis. *J Cancer Mol* **2006,** *2*, (3), 101-106.

(6) Solinas, G.; Germano, G.; Mantovani, A.; Allavena, P. Tumor-associated macrophages (TAM) as major players of the cancer-related inflammation. *J Leukoc Biol* **2009,** *86*, (5), 1065-73.

(7) Lewis, C. E.; Pollard, J. W. Distinct role of macrophages in different tumor microenvironments. *Cancer Res* **2006,** *66*, (2), 605-12.

(8) Feurino, L. W.; Fisher, W. E.; Bharadwaj, U.; Yao, Q.; Chen, C.; Li, M. Current update of cytokines in pancreatic cancer: pathogenic mechanisms, clinical indication, and therapeutic values. *Cancer Invest* **2006,** *24*, (7), 696-703.

(9) Lin, E. Y.; Nguyen, A. V.; Russell, R. G.; Pollard, J. W. Colony-stimulating factor 1 promotes progression of mammary tumors to malignancy. *J Exp Med* **2001,** *193*, (6), 727-40.

(10) Lin, E. Y.; Li, J. F.; Gnatovskiy, L.; Deng, Y.; Zhu, L.; Grzesik, D. A.; Qian, H.; Xue, X. N.; Pollard, J. W. Macrophages regulate the angiogenic switch in a mouse model of breast cancer. *Cancer Res* **2006,** *66*, (23), 11238-46.

(11) Clark, C. E.; Hingorani, S. R.; Mick, R.; Combs, C.; Tuveson, D. A.; Vonderheide, R. H. Dynamics of the immune reaction to pancreatic cancer from inception to invasion. *Cancer Res* **2007,** *67*, (19), 9518-27.

(12) Gardian, K.; Janczewska, S.; Olszewski, W. L.; Durlik, M. Analysis of Pancreatic Cancer Microenvironment: Role of Macrophage Infiltrates and Growth Factors Expression. *J Cancer* **2012,** *3*, 285-291.

(13) Esposito, I.; Menicagli, M.; Funel, N.; Bergmann, F.; Boggi, U.; Mosca, F.; Bevilacqua, G.; Campani, D. Inflammatory cells contribute to the generation of an angiogenic phenotype in pancreatic ductal adenocarcinoma. *J Clin Pathol* **2004,** *57*, (6), 630-6.

(14) Kuwahara, K.; Sasaki, T.; Kuwada, Y.; Murakami, M.; Yamasaki, S.; Chayama, K. Expressions of angiogenic factors in pancreatic ductal carcinoma: a correlative study with clinicopathologic parameters and patient survival. *Pancreas* **2003,** *26*, (4), 344-9.

(15) Varney, M. L.; Johansson, S. L.; Singh, R. K. Tumour-associated macrophage infiltration, neovascularization and aggressiveness in malignant melanoma: role of monocyte chemotactic protein-1 and vascular endothelial growth factor-A. *Melanoma Res* **2005,** *15*, (5), 417-25.

(16) Elgert, K. D.; Alleva, D. G.; Mullins, D. W. Tumor-induced immune dysfunction: the macrophage connection. *J Leukoc Biol* **1998,** *64*, (3), 275-90.

(17) Groblewska, M.; Mroczko, B.; Wereszczynska-Siemiatkowska, U.; Mysliwiec, P.; Kedra, B.; Szmitkowski, M. Serum levels of granulocyte colony-stimulating factor (G-CSF) and macrophage colony-stimulating factor (M-CSF) in pancreatic cancer patients. *Clin Chem Lab Med* **2007,** *45*, (1), 30-4.

(18) Kubota, Y.; Takubo, K.; Shimizu, T.; Ohno, H.; Kishi, K.; Shibuya, M.; Saya, H.; Suda, T. M-CSF inhibition selectively targets pathological angiogenesis and lymphangiogenesis. *J Exp Med* **2009,** *206*, (5), 1089-102.

(19) Zhu, Y.; Knolhoff, B. L.; Meyer, M. A.; Nywening, T. M.; West, B. L.; Luo, J.; Wang-Gillam, A.; Goedegebuure, S. P.; Linehan, D. C.; DeNardo, D. G. CSF1/CSF1R Blockade Reprograms Tumor-Infiltrating Macrophages and Improves Response to T-cell Checkpoint Immunotherapy in Pancreatic Cancer Models. *Cancer Res* **2014,** *74*, (18), 5057-69.

(20) Komohara, Y.; Fujiwara, Y.; Ohnishi, K.; Takeya, M. Tumor-associated macrophages: Potential therapeutic targets for anti-cancer therapy. *Adv Drug Deliv Rev* **2016,** *99*, (Pt B), 180-5.

(21) Jinushi, M.; Komohara, Y. Tumor-associated macrophages as an emerging target against tumors: Creating a new path from bench to bedside. *Biochim Biophys Acta* **2015,** *1855*, (2), 123-30.

(22) Bowman, R. L.; Joyce, J. A. Therapeutic targeting of tumor-associated macrophages and microglia in glioblastoma. *Immunotherapy* **2014,** *6*, (6), 663-6.

(23) Colonna, M.; Facchetti, F. TREM-1 (triggering receptor expressed on myeloid cells): a new player in acute inflammatory responses. *J Infect Dis* **2003,** *187 Suppl 2*, S397-401.

(24) Wang, D. Y.; Qin, R. Y.; Liu, Z. R.; Gupta, M. K.; Chang, Q. Expression of TREM-1 mRNA in acute pancreatitis. *World J Gastroenterol* **2004,** *10*, (18), 2744-6.

(25) Lagler, H.; Sharif, O.; Haslinger, I.; Matt, U.; Stich, K.; Furtner, T.; Doninger, B.; Schmid, K.; Gattringer, R.; de Vos, A. F.; Knapp, S. TREM-1 activation alters the dynamics of pulmonary IRAK-M expression in vivo and improves host defense during pneumococcal pneumonia. *J Immunol* **2009,** *183*, (3), 2027-36.

(26) Schenk, M.; Bouchon, A.; Seibold, F.; Mueller, C. TREM-1--expressing intestinal macrophages crucially amplify chronic inflammation in experimental colitis and inflammatory bowel diseases. *J Clin Invest* **2007,** *117*, (10), 3097-106.

(27) Sigalov, A. B. A novel ligand-independent peptide inhibitor of TREM-1 suppresses tumor growth in human lung cancer xenografts and prolongs survival of mice with lipopolysaccharide-induced septic shock. *Int Immunopharmacol* **2014,** *21*, (1), 208-219.

(28) Yako, Y. Y.; Kruger, D.; Smith, M.; Brand, M. Cytokines as Biomarkers of Pancreatic Ductal Adenocarcinoma: A Systematic Review. *PLoS One* **2016,** *11*, (5), e0154016.

(29) Tjomsland, V.; Spangeus, A.; Valila, J.; Sandstrom, P.; Borch, K.; Druid, H.; Falkmer, S.; Falkmer, U.; Messmer, D.; Larsson, M. Interleukin 1alpha sustains the expression of inflammatory factors in human pancreatic cancer microenvironment by targeting cancer-associated fibroblasts. *Neoplasia* **2011,** *13*, (8), 664-75.

(30) Pelham, C. J.; Agrawal, D. K. Emerging roles for triggering receptor expressed on myeloid cells receptor family signaling in inflammatory diseases. *Expert Rev Clin Immunol* **2014,** *10*, (2), 243-56.

(31) Shen, Z. T.; Sigalov, A. B. Rationally designed ligand-independent peptide inhibitors of TREM-1 ameliorate collagen-induced arthritis. *J Cell Mol Med* **2017**, in press.

(32) Weber, B.; Schuster, S.; Zysset, D.; Rihs, S.; Dickgreber, N.; Schurch, C.; Riether, C.; Siegrist, M.; Schneider, C.; Pawelski, H.; Gurzeler, U.; Ziltener, P.; Genitsch, V.; Tacchini-Cottier, F.; Ochsenbein, A.; Hofstetter, W.; Kopf, M.; Kaufmann, T.; Oxenius, A.; Reith, W.; Saurer, L.; Mueller, C. TREM-1 Deficiency Can Attenuate Disease Severity without Affecting Pathogen Clearance. *PLoS Pathog* **2014,** *10*, (1), e1003900.

(33) Ho, C. C.; Liao, W. Y.; Wang, C. Y.; Lu, Y. H.; Huang, H. Y.; Chen, H. Y.; Chan, W. K.; Chen, H. W.; Yang, P. C. TREM-1 expression in tumor-associated macrophages and clinical outcome in lung cancer. *Am J Respir Crit Care Med* **2008,** *177*, (7), 763-70.

(34) Read, C. B.; Kuijper, J. L.; Hjorth, S. A.; Heipel, M. D.; Tang, X.; Fleetwood, A. J.; Dantzler, J. L.; Grell, S. N.; Kastrup, J.; Wang, C.; Brandt, C. S.; Hansen, A. J.; Wagtmann, N. R.; Xu, W.; Stennicke, V. W. Cutting Edge: identification of neutrophil PGLYRP1 as a ligand for TREM-1. *J Immunol* **2015,** *194*, (4), 1417-21.

(35) Sigalov, A. B. Multichain immune recognition receptor signaling: different players, same game? *Trends Immunol* **2004,** *25*, (11), 583-9.

(36) Sigalov, A. B. Immune cell signaling: a novel mechanistic model reveals new therapeutic targets. *Trends Pharmacol Sci* **2006,** *27*, (10), 518-24.

(37) Shen, Z. T.; Sigalov, A. B. SARS Coronavirus Fusion Peptide-Derived Sequence Suppresses Collagen-Induced Arthritis in DBA/1J Mice. *Sci Rep* **2016,** *6*, 28672.

(38) Shen, Z. T.; Zheng, S.; Gounis, M. J.; Sigalov, A. B. Diagnostic Magnetic Resonance Imaging of Atherosclerosis in Apolipoprotein E Knockout Mouse Model Using Macrophage-Targeted Gadolinium-Containing Synthetic Lipopeptide Nanoparticles. *PLoS One* **2015,** *10*, (11), e0143453.

(39) Sigalov, A. B. Nature-inspired nanoformulations for contrast-enhanced in vivo MR imaging of macrophages. *Contrast Media Mol Imaging* **2014,** *9*, (5), 372-82.

(40) Gupta, S.; Jain, A.; Chakraborty, M.; Sahni, J. K.; Ali, J.; Dang, S. Oral delivery of therapeutic proteins and peptides: a review on recent developments. *Drug Deliv* **2013,** *20*, (6), 237-46.

(41) Furman, R. H.; Sanbar, S. S.; Alaupovic, P.; Bradford, R. H.; Howard, R. P. Studies of the Metabolism of Radioiodinated Human Serum Alpha Lipoprotein in Normal and Hyperlipidemic Subjects. *J Lab Clin Med* **1964,** *63*, 193-204.

(42) Condeelis, J.; Pollard, J. W. Macrophages: obligate partners for tumor cell migration, invasion, and metastasis. *Cell* **2006,** *124*, (2), 263-6.

(43) Zumsteg, A.; Baeriswyl, V.; Imaizumi, N.; Schwendener, R.; Ruegg, C.; Christofori, G. Myeloid cells contribute to tumor lymphangiogenesis. *PLoS One* **2009,** *4*, (9), e7067.

(44) Wang, D.; Stockard, C. R.; Harkins, L.; Lott, P.; Salih, C.; Yuan, K.; Buchsbaum, D.; Hashim, A.; Zayzafoon, M.; Hardy, R. W.; Hameed, O.; Grizzle, W.; Siegal, G. P. Immunohistochemistry in the evaluation of neovascularization in tumor xenografts. *Biotech Histochem* **2008,** *83*, (3-4), 179-89.

(45) Pieramici, D. J.; Rabena, M. D. Anti-VEGF therapy: comparison of current and future agents. *Eye (Lond)* **2008,** *22*, (10), 1330-6.

(46) Kumari, N.; Dwarakanath, B. S.; Das, A.; Bhatt, A. N. Role of interleukin-6 in cancer progression and therapeutic resistance. *Tumour Biol* **2016,** *37*, (9), 11553-11572.

(47) Mitchem, J. B.; Brennan, D. J.; Knolhoff, B. L.; Belt, B. A.; Zhu, Y.; Sanford, D. E.; Belaygorod, L.; Carpenter, D.; Collins, L.; Piwnica-Worms, D.; Hewitt, S.; Udupi, G. M.; Gallagher, W. M.; Wegner, C.; West, B. L.; Wang-Gillam, A.; Goedegebuure, P.; Linehan, D. C.; DeNardo, D. G. Targeting tumor-infiltrating macrophages decreases tumor-initiating cells, relieves immunosuppression, and improves chemotherapeutic responses. *Cancer Res* **2013,** *73*, (3), 1128-41.

(48) Julovi, S. M.; Xue, A.; Thanh, L. T.; Gill, A. J.; Bulanadi, J. C.; Patel, M.; Waddington, L. J.; Rye, K. A.; Moghaddam, M. J.; Smith, R. C. Apolipoprotein A-II Plus Lipid Emulsion Enhance Cell Growth via SR-B1 and Target Pancreatic Cancer In Vitro and In Vivo. *PLoS One* **2016,** *11*, (3), e0151475.

(49) Liu, T.; Krieger, M.; Kan, H. Y.; Zannis, V. I. The effects of mutations in helices 4 and 6 of ApoA-I on scavenger receptor class B type I (SR-BI)-mediated cholesterol efflux suggest that formation of a productive complex between reconstituted high density lipoprotein and SR-BI is required for efficient lipid transport. *J Biol Chem* **2002,** *277*, (24), 21576-84.

(50) Sigalov, A. B. Novel mechanistic concept of platelet inhibition. *Expert Opin Ther Targets* **2008,** *12*, (6), 677-92.

(51) Wang, X. M.; Djordjevic, J. T.; Bender, V.; Manolios, N. T cell antigen receptor (TCR) transmembrane peptides colocalize with TCR, not lipid rafts, in surface membranes. *Cell Immunol* **2002,** *215*, (1), 12-9.

(52) Sigalov, A. B. Novel mechanistic insights into viral modulation of immune receptor signaling. *PLoS Pathog* **2009,** *5*, (7), e1000404.

FIGURE CAPTIONS

Figure 1 The proposed role of inhibition of TREM-1 expressed on tumor-associated macrophages (TAMs) in pancreatic cancer. (A) Pancreatic ductal adenocarcinoma cells, cancer-associated fibroblasts (CAFs) and TAMs play a major role in generating a tumor favorable microenvironment, in part by producing such cytokines and growth factors as interleukin (IL)-1α, IL-6 and macrophage colony-stimulating factor (M-CSF). (B) Novel TREM-1 peptide inhibitors are rationally designed using the SCHOOL approach to inhibit TREM-1 in a ligand-independent manner by blocking transmembrane interactions between TREM-1 and its signaling partner DAP-12. These SCHOOL peptides can be employed in either free form or incorporated into macrophage-targeted particles, which allows them to reach their site of action from either outside (Route 1) or inside the cell (Route 2).

Figure 2 Treatment with free or high density lipoprotein (HDL)-bound GF9 suppresses tumor growth in experimental pancreatic cancer without affecting body weight. (A and B) As described in the Materials and Methods, after tumors in AsPC-1-, BxPC-3- or Capan-1-bearing mice reached a volume of 150-200 mm^3, mice were randomized into groups and intraperitoneally (i.p.) administered once daily 5 times per week (5qw) with either vehicle (black diamonds), GF9 (dark gray squares), GF9-loaded discoidal HDL (GF9-dHDL, light gray circles) or GF9-loaded spherical HDL (GF9-sHDL, white circles) at indicated doses. Treatment persisted for 31, 29 and 29 days for mice containing AsPC-1, BxPC-3 and Capan-1 tumor xenografts, respectively. Mean tumor volumes are calculated and plotted in A. Body weights are plotted in B. All results are expressed as the mean ± SEM (n = 6 mice per group). On the final day of treatment, tumor volumes and body weights were compared between the

drug-treated and control groups. **, $p < 0.01$; ***, $p < 0.001$; ****, $p < 0.0001$ (versus vehicle).

Figure 3 Treatment with high density lipoprotein (HDL)-bound 31-mer peptides GA31 and GE31 suppresses tumor growth in experimental pancreatic cancer without affecting body weight. (A and B) As described in the Materials and Methods, after tumors in AsPC-1-, BxPC-3- or Capan-1-bearing mice reached a calculated volume of 150-200 mm^3, mice were randomized into groups and intraperitoneally (i.p.) administered once daily 5 times per week (5qw) with either vehicle (black diamonds), discoidal HDL (dHDL) loaded with an equimolar mixture of GA31 and GE31 (GA/E31-dHDL, light gray triangles) or spherical HDL (sHDL) loaded with an equimolar mixture of GA31 and GE31 (GA/E31-sHDL, white triangles) at indicated doses. Treatment persisted for 31, 29 and 29 days for mice containing AsPC-1, BxPC-3 and Capan-1 tumor xenografts, respectively. Mean tumor volumes are calculated and plotted in A. Body weights are plotted in B. All results are expressed as the mean ± SEM (n = 6 mice per group). On the final day of treatment, tumor volumes and body weights were compared between the drug-treated and control groups. ***, $p < 0.001$; ****, $p < 0.0001$ (versus vehicle).

Figure 4 Treatment with free or high density lipoprotein (HDL)-bound SCHOOL TREM-1 inhibitory GF9 sequences prolongs survival in experimental pancreatic cancer. (A and B) Kaplan-Meier survival curves are shown for AsPC-1-, BxPC-3- or Capan-1-bearing mice (n = 6 mice per group) treated using free and HDL-bound SCHOOL TREM-1 inhibitory GF9 sequences as described in the legends to Figures 2 and 3. **, $p < 0.01$; ***, $p < 0.001$ by log-rank test (versus vehicle).

Figure 5 TREM-1 inhibition suppresses intratumoral macrophage infiltration in experimental pancreatic cancer. (A) Antitumor activity expressed as % T/C was plotted against the intratumoral macrophage content for groups of AsPC-1-, BxPC-3- and Capan-1-bearing mice (n = 4 mice per group) treated with free and high density lipoprotein (HDL)-bound SCHOOL TREM-1 inhibitory GF9 sequences. (B and C) As described in the Materials and Methods, tumors from AsPC-1-, BxPC-3- and Capan-1-bearing mice treated using either vehicle (black bars), GF9 (dark gray bars), GF9-loaded spherical HDL (GF9-sHDL, light gray bars) or sHDL loaded with an equimolar mixture of GA31 and GE31 (GA/E31-sHDL, white bars) were collected at the end of the study, sectioned and stained for macrophages using F4/80 antibodies. (B) F4/80 staining was quantified as described in the Materials and Methods. Results are expressed as the mean ± SEM (n = 4 mice per group). *, $p < 0.05$; **, $p < 0.01$ (versus vehicle). (C) Representative F4/80 images from BxPC-3-bearing mice treated using free and HDL-bound SCHOOL TREM-1 inhibitory GF9 sequences. Scale bar = 200 μm.

Figure 6 TREM-1 inhibition suppresses serum proinflammatory cytokines in xenograft mouse models of pancreatic cancer. Serum interleukin-1α (IL-1α), IL-6 and macrophage colony-stimulating factor (M-CSF) levels were analyzed on study days 1 and 8 in AsPC-1-, BxPC-3- and Capan-1-bearing mice treated using either vehicle (black diamonds), GF9 (dark gray squares) or GF9-loaded spherical high density lipoproteins (GF9-sHDL, white circles). Results are expressed as the mean ± SEM (n = 5 mice per group). *, $p < 0.05$; **, $p < 0.01$; ***, $p < 0.001$; ****, $p < 0.0001$ (versus vehicle).

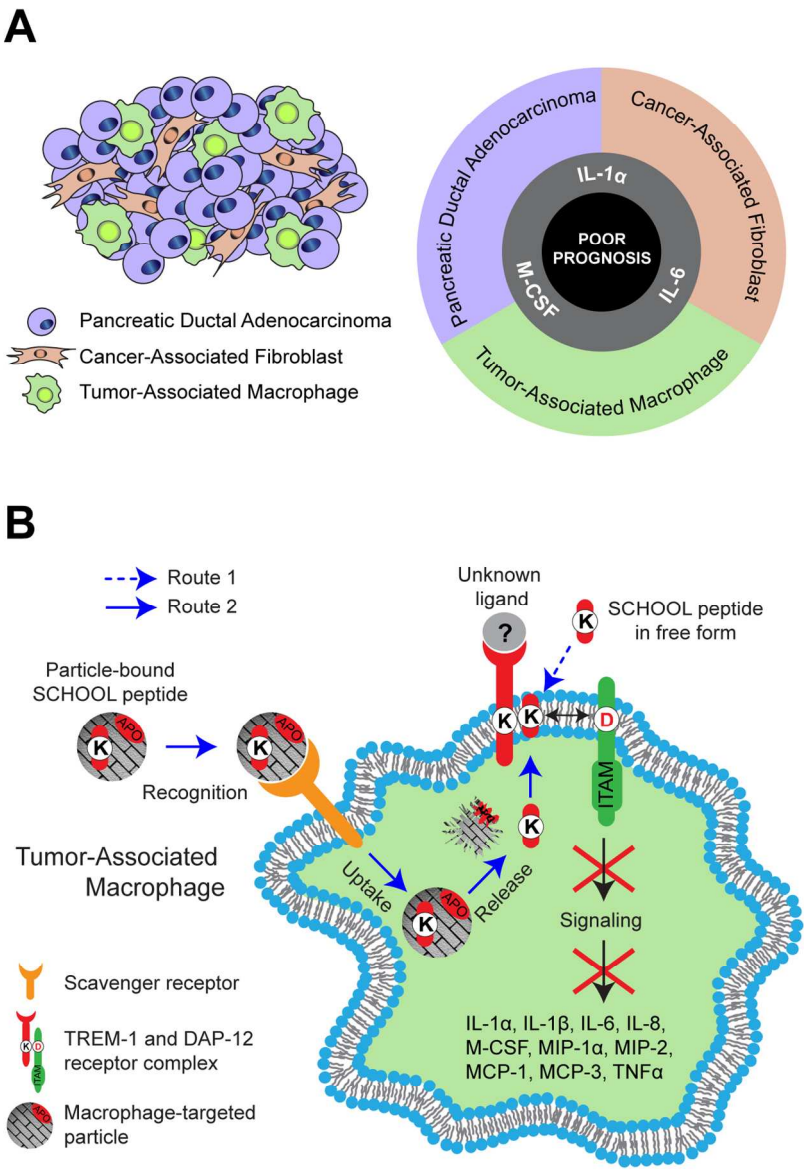

Figure 1 The proposed role of inhibition of TREM-1 expressed on tumor-associated macrophages (TAMs) in pancreatic cancer. (A) Pancreatic ductal adenocarcinoma cells, cancer-associated fibroblasts (CAFs) and TAMs play a major role in generating a tumor favorable microenvironment, in part by producing such cytokines and growth factors as interleukin (IL)-1α, IL-6 and macrophage colony-stimulating factor (M-CSF). (B) Novel TREM-1 peptide inhibitors are rationally designed using the SCHOOL approach to inhibit TREM-1 in a ligand-independent manner by blocking transmembrane interactions between TREM-1 and its signaling partner DAP-12. These SCHOOL peptides can be employed in either free form or incorporated into macrophage-targeted particles, which allows them to reach their site of action from either outside (Route 1) or inside the cell (Route 2).

114x168mm (300 x 300 DPI)

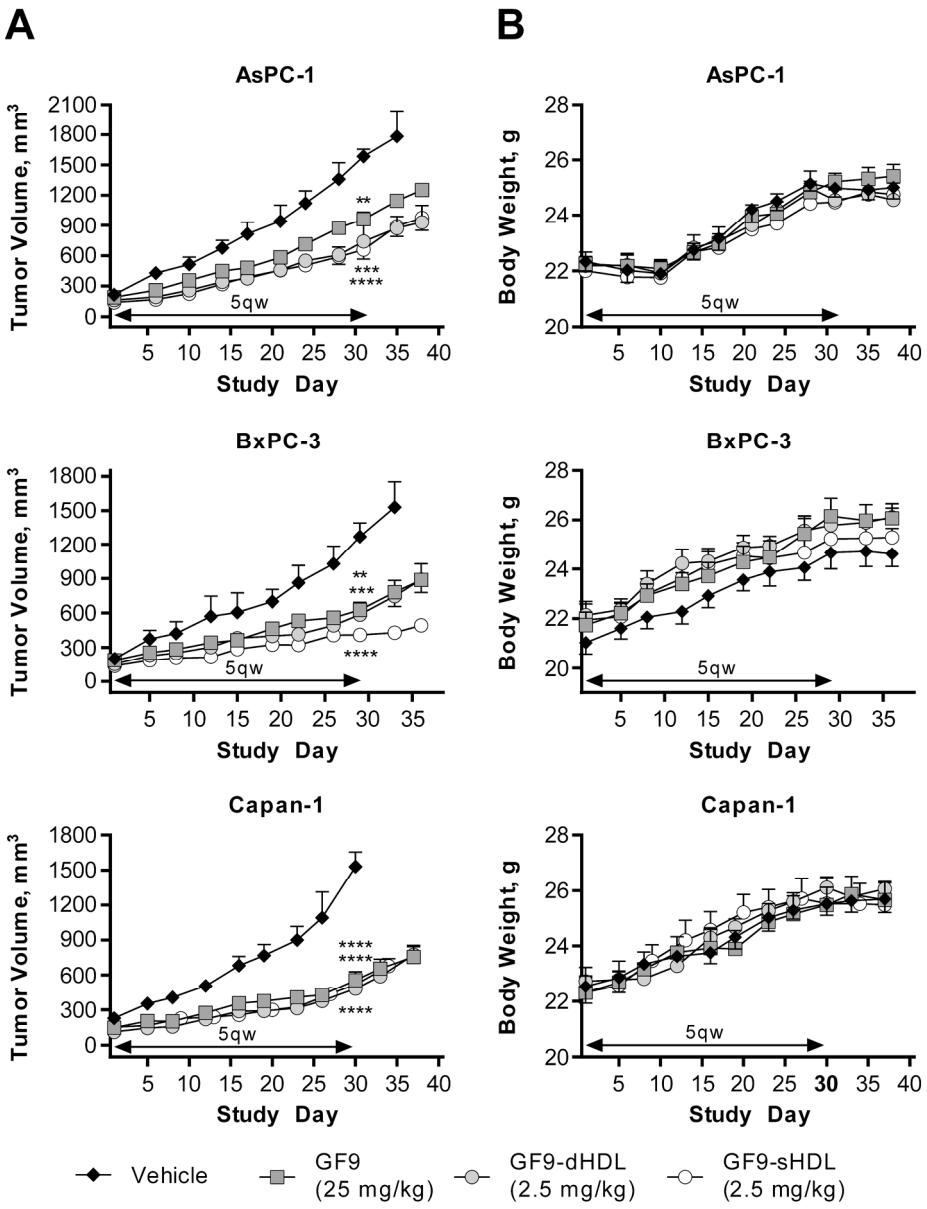

Figure 2 Treatment with free or high density lipoprotein (HDL)-bound GF9 suppresses tumor growth in experimental pancreatic cancer without affecting body weight. (A and B) As described in the Materials and Methods, after tumors in AsPC-1-, BxPC-3- or Capan-1-bearing mice reached a volume of 150-200 mm^3, mice were randomized into groups and intraperitoneally (i.p.) administered once daily 5 times per week (5qw) with either vehicle (black diamonds), GF9 (dark gray squares), GF9-loaded discoidal HDL (GF9-dHDL, light gray circles) or GF9-loaded spherical HDL (GF9-sHDL, white circles) at indicated doses. Treatment persisted for 31, 29 and 29 days for mice containing AsPC-1, BxPC-3 and Capan-1 tumor xenografts, respectively. Mean tumor volumes are calculated and plotted in A. Body weights are plotted in B. All results are expressed as the mean ± SEM (n = 6 mice per group). On the final day of treatment, tumor volumes and body weights were compared between the drug-treated and control groups. **, $p < 0.01$; ***, $p < 0.001$; ****, $p < 0.0001$ (versus vehicle).

182x239mm (300 x 300 DPI)

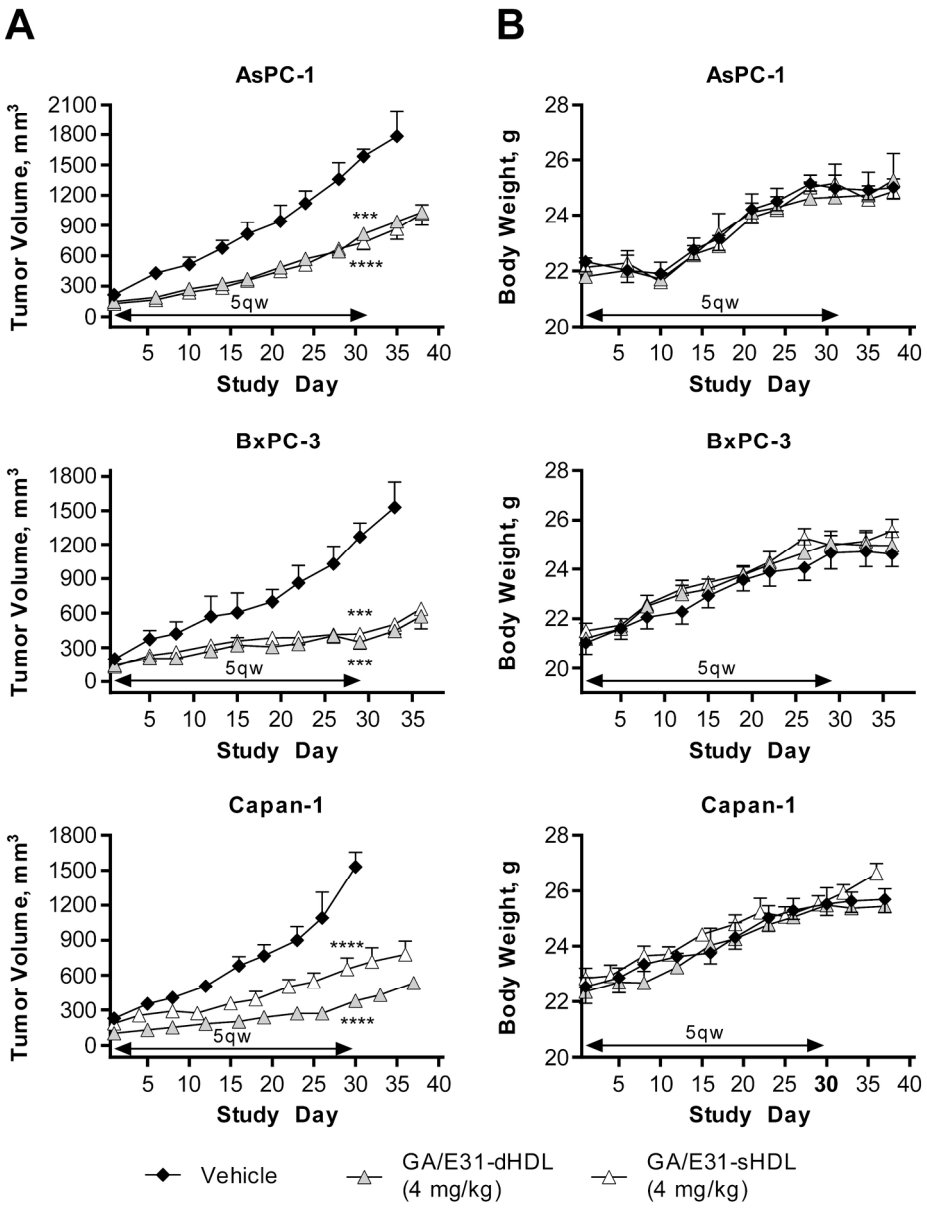

Figure 3 Treatment with high density lipoprotein (HDL)-bound 31-mer peptides GA31 and GE31 suppresses tumor growth in experimental pancreatic cancer without affecting body weight. (A and B) As described in the Materials and Methods, after tumors in AsPC-1-, BxPC-3- or Capan-1-bearing mice reached a calculated volume of 150-200 mm^3, mice were randomized into groups and intraperitoneally (i.p.) administered once daily 5 times per week (5qw) with either vehicle (black diamonds), discoidal HDL (dHDL) loaded with an equimolar mixture of GA31 and GE31 (GA/E31-dHDL, light gray triangles) or spherical HDL (sHDL) loaded with an equimolar mixture of GA31 and GE31 (GA/E31-sHDL, white triangles) at indicated doses. Treatment persisted for 31, 29 and 29 days for mice containing AsPC-1, BxPC-3 and Capan-1 tumor xenografts, respectively. Mean tumor volumes are calculated and plotted in A. Body weights are plotted in B. All results are expressed as the mean ± SEM (n = 6 mice per group). On the final day of treatment, tumor volumes and body weights were compared between the drug-treated and control groups. ***, $p < 0.001$; ****, $p < 0.0001$ (versus vehicle).

182x238mm (300 x 300 DPI)

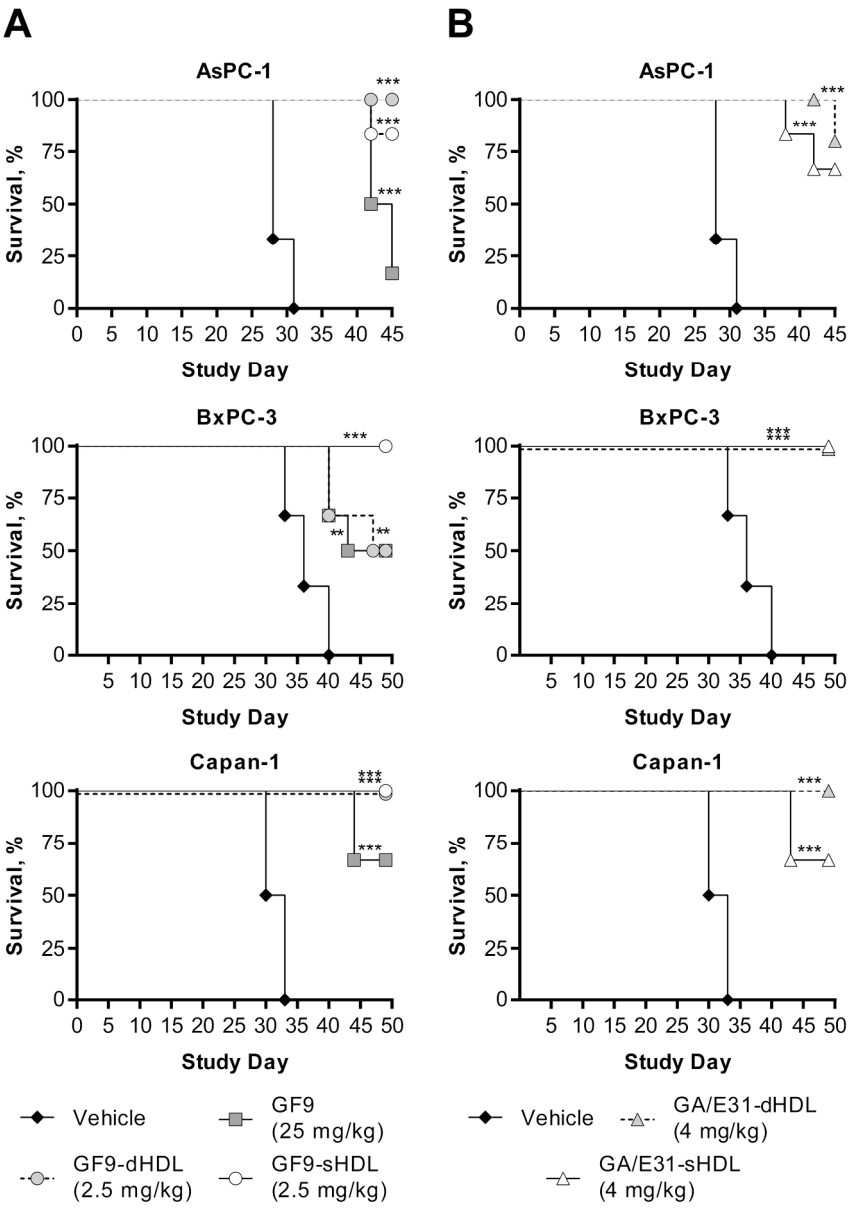

Figure 4 Treatment with free or high density lipoprotein (HDL)-bound SCHOOL TREM-1 inhibitory GF9 sequences prolongs survival in experimental pancreatic cancer. (A and B) Kaplan-Meier survival curves are shown for AsPC-1-, BxPC-3- or Capan-1-bearing mice (n = 6 mice per group) treated using free and HDL-bound SCHOOL TREM-1 inhibitory GF9 sequences as described in the legends to Figures 2 and 3. **, $p < 0.01$; ***, $p < 0.001$ by log-rank test (versus vehicle).

193x274mm (300 x 300 DPI)

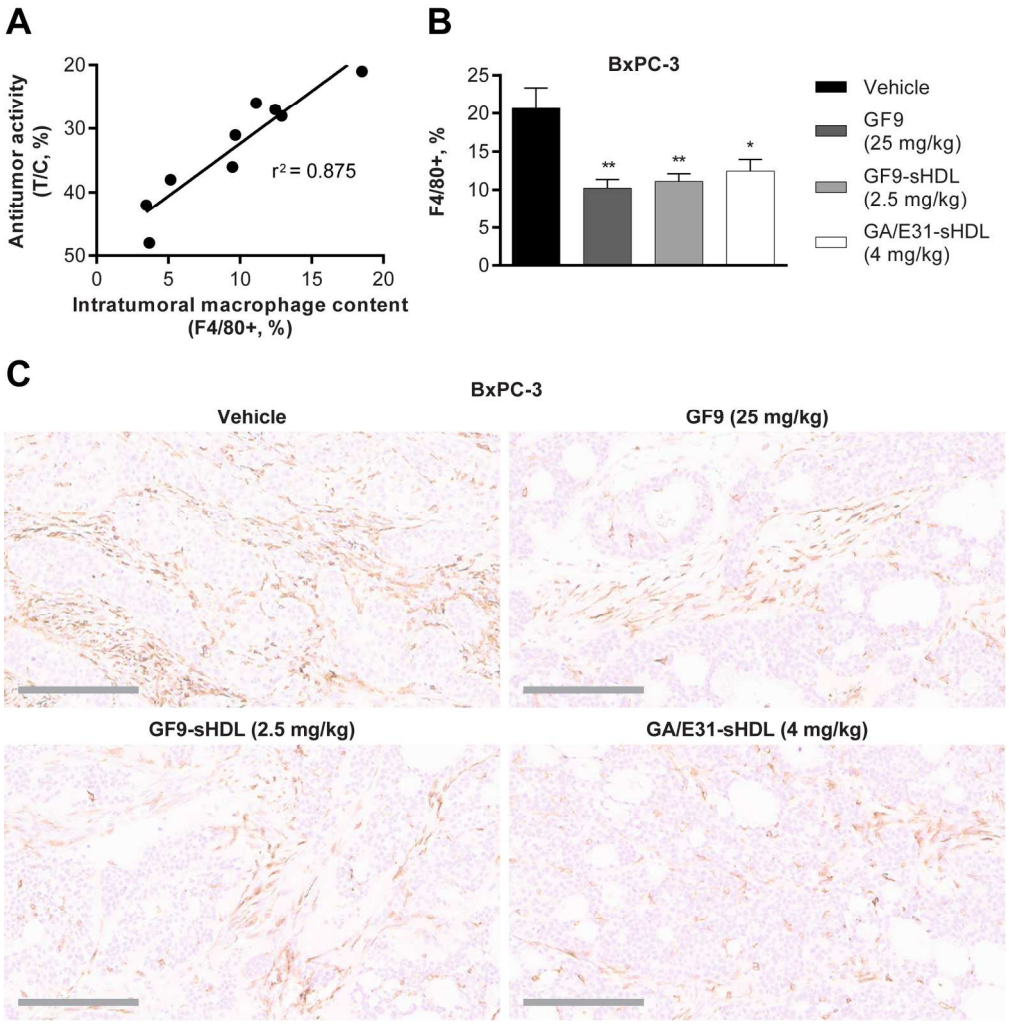

Figure 5 TREM-1 inhibition suppresses intratumoral macrophage infiltration in experimental pancreatic cancer. (A) Antitumor activity expressed as % T/C was plotted against the intratumoral macrophage content for groups of AsPC-1-, BxPC-3- and Capan-1- bearing mice (n = 4 mice per group) treated with free and high density lipoprotein (HDL)-bound SCHOOL TREM-1 inhibitory GF9 sequences. (B and C) As described in the Materials and Methods, tumors from AsPC-1-, BxPC-3- and Capan-1-bearing mice treated using either vehicle (black bars), GF9 (dark gray bars), GF9-loaded spherical HDL (GF9-sHDL, light gray bars) or sHDL loaded with an equimolar mixture of GA31 and GE31 (GA/E31-sHDL, white bars) were collected at the end of the study, sectioned and stained for macrophages using F4/80 antibodies. (B) F4/80 staining was quantified as described in the Materials and Methods. Results are expressed as the mean ± SEM (n = 4 mice per group). *, $p < 0.05$; **, $p < 0.01$ (versus vehicle). (C) Representative F4/80 images from BxPC-3-bearing mice treated using free and HDL-bound SCHOOL TREM-1 inhibitory GF9 sequences. Scale bar = 200 μm.

177x180mm (300 x 300 DPI)

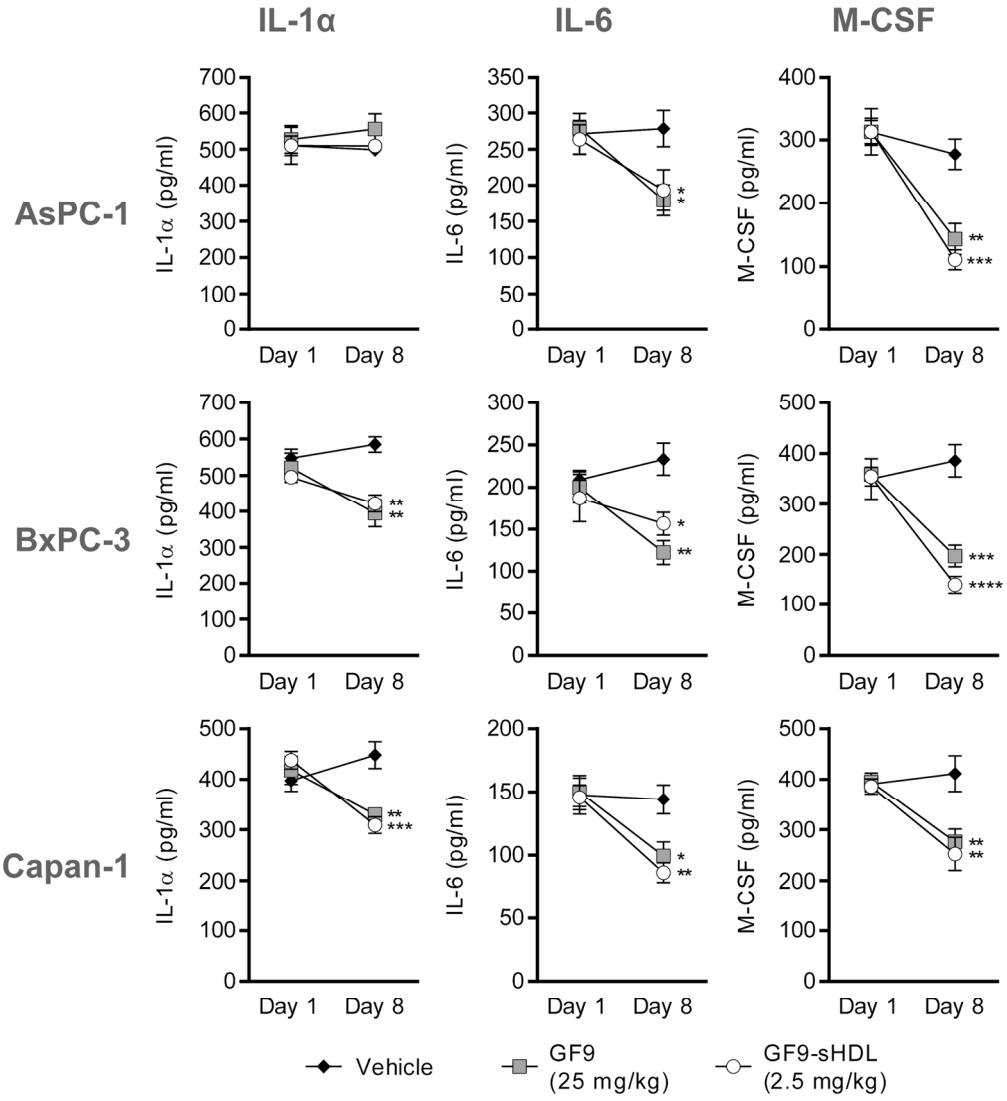

Figure 6 TREM-1 inhibition suppresses serum proinflammatory cytokines in xenograft mouse models of pancreatic cancer. Serum interleukin-1α (IL-1α), IL-6 and macrophage colony-stimulating factor (M-CSF) levels were analyzed on study days 1 and 8 in AsPC-1-, BxPC-3- and Capan-1-bearing mice treated using either vehicle (black diamonds), GF9 (dark gray squares) or GF9-loaded spherical high density lipoproteins (GF9-sHDL, white circles). Results are expressed as the mean ± SEM (n = 5 mice per group). *, $p < 0.05$; **, $p < 0.01$; ***, $p < 0.001$; ****, $p < 0.0001$ (versus vehicle).

164x179mm (300 x 300 DPI)

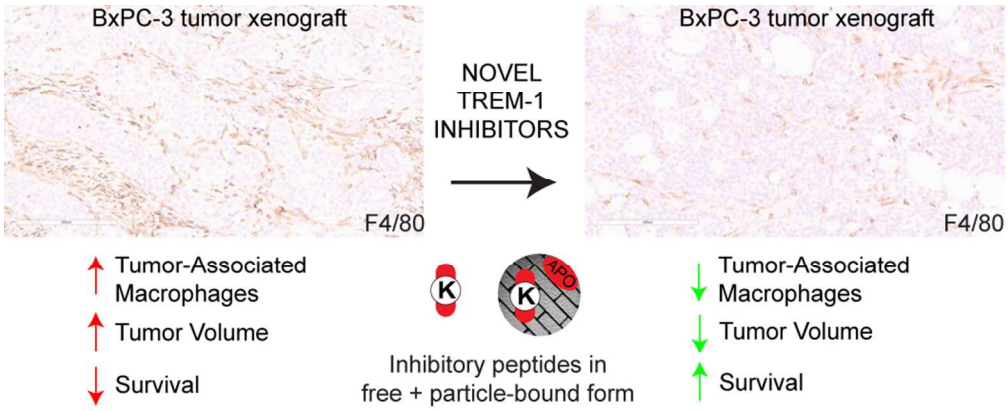

Graphical abstract

89x38mm (300 x 300 DPI)